

Elsevier Editorial System(tm) for Computer Methods and Programs in Biomedicine
Manuscript Draft

Manuscript Number:

Title: TUBERCULINE REACTION MEASURED BY INFRARED THERMOGRAPHY

Article Type: Full Length Article

Section/Category: Section II: Systems and Programs

Keywords: Tuberculin test; Infrared Thermography; Image processing

Corresponding Author: Prof. Marcos Faundez-Zanuy,

Corresponding Author's Institution: Fundació Tecnocampus

First Author: José Antonio Fiz, PhD

Order of Authors: José Antonio Fiz, PhD; Manuel Lozano; Enrique Monte-Moreno, PhD; Adela Gonzalez-Martinez; Laura Rodriguez-Pons; Caroline Becker; Marcos Faundez-Zanuy; Juan Ruiz-Manzano, PhD

Abstract: Setting: The infection with Mycobacterium tuberculosis gives a delayed immune response, measured by the tuberculin skin test. We present a new technique for evaluation based on automatic detection and measurement of skin infrared emission.

Design: 21 subjects (57.0±17.8 yr), (7/14, M/F) with suspected tuberculosis contact were examined with an IR thermal camera, 48 hours after skin injection.

Results: In 15 subjects, IR analysis was positive for tuberculin test. Mean temperature of injection area was higher, around 1 °C, for the positive group (36.0± 0.3 °C positive group; 35.2±1.7 °C negative group, p<0.001, Non parametric U Mann-Whitney Test).

Conclusion: IR may represent an improved estimation of tuberculosis infection, given that it does not depend on reader variability and measures the increase of heat irradiation produced by the allergic tuberculin response.

Suggested Reviewers: Jiri Mekyska PhD
Associate Professor, Brno University of Technology (Czech Republic)
j.mekyska@gmail.com
Expert in biomedical applications and thermal imaging

Carlo Morabito PhD
vice-rector, University Reggio Calabria (Italy)
morabito@unirc.it
Expert in soft computing systems and biomedical applications

Anna Esposito PhD
professor, University of Naples
Anna.ESPOSITO@unina2.it
Expert in computer science and thermal imaging

Jordi Sole-Casals PhD

Associate Professor, University of Vic
jordi.sole@uvic.cat
Expert in biomedical applications and signal processing

Opposed Reviewers:

We declare no conflict of interests.

The authors

25/2/2015

TUBERCULINE REACTION MEASURED BY INFRARED THERMOGRAPHY

José Antonio Fiz ^{1,3*} (jafiz@msn.com) (JAF)	MD, PhD
Manuel Lozano ² (mlozanogar@gmail.com) (ML)	Engineer
Enrique Monte-Moreno ³ (enric.monte@upc.edu) (EM)	Engineer, PhD
Adela Gonzalez-Martinez ¹ (agonzalezm.germanstrias@gencat.cat) (AG)	Technician
Laura Rodriguez Pons ¹ (laurarodriguezpons@gmail.com) (LR)	MD
Caroline Becker ¹ (arialcb@gmail.com) (CB)	MD
Marcos Faundez-Zanuy ⁴ (faundez@tecnocampus.cat) (MF)	Engineer, PhD
Juan Ruiz Manzano ¹ (jruizmanzano.germanstrias@gencat.cat) (JR)	MD, PhD

¹ Pulmonology Department, Germans Trias I Pujol University Hospital. 8th, Carretera del Canyet s/n. 08916, Badalona, Spain. Phone Number

² Innovation Group, Health Sciences Research Institute of Germans Trias i Pujol Foundation(IGTIP). Ctra, de Can Ruti /Camí de les escoles s/n, 08916, Badalona, Spain.

³ Center for Language and Speech Technologies and Applications (TALP), Technical University of Catalunya (UPC), Jordi Girona, 1-3, S112, Campus Nord, Barcelona, Spain.

⁴Escola Superior Politècnica Tecnocampus Mataró. Spain Phone Number: 34 93 169 65 01

Running head: Tuberculin test measured by Infrared Thermography

Word Count: 3046

Keywords: Tuberculin test, Infrared Thermography

Corresponding author: Dr José Antonio Fiz

ABSTRACT

Setting: The infection with *Mycobacterium tuberculosis* gives a delayed immune response, measured by the tuberculin skin test. We present a new technique for evaluation based on automatic detection and measurement of skin infrared emission.

Design: 21 subjects (57.0 ± 17.8 yr), (7/14, M/F) with suspected tuberculosis contact were examined with an IR thermal camera, 48 hours after skin injection.

Results: In 15 subjects, IR analysis was positive for tuberculin test. Mean temperature of injection area was higher, around 1 °C, for the positive group (36.0 ± 0.3 °C positive group; 35.2 ± 1.7 °C negative group, $p < 0.001$, Non parametric U Mann-Whitney Test).

Conclusion: IR may represent an improved estimation of tuberculosis infection, given that it does not depend on reader variability and measures the increase of heat irradiation produced by the allergic tuberculin response.

Highlights

- First paper devoted to tuberculine reaction measurement based on thermal imaging.
- Proposed method alleviates the variability of a human supervisor
- Low cost system for solving a challenging diagnose

TUBERCULINE REACTION MEASURED BY INFRARED THERMOGRAPHY

José Antonio Fiz^{1,3*} (jafiz@msn.com) (JAF) MD, PhD

Manuel Lozano² (mlozanogar@gmail.com) (ML) Engineer

Enrique Monte-Moreno³ (enric.monte@upc.edu) (EM) Engineer, PhD

Adela Gonzalez-Martinez¹ (agonzalezm.germanstrias@gencat.cat) (AG) Technician

Laura Rodriguez Pons¹ (laurarodriguezpons@gmail.com) (LR) MD

Caroline Becker¹ (arialcb@gmail.com) (CB) MD

Marcos Faundez-Zanuy⁴ (faundez@tecnocampus.cat) (MF) Engineer, PhD

Juan Ruiz Manzano¹ (jruizmanzano.germanstrias@gencat.cat) (JR) MD, PhD

¹ Pulmonology Department, Germans Trias I Pujol University Hospital. 8th, Carretera del Canyet s/n. 08916, Badalona, Spain. Phone Number

² Innovation Group, Health Sciences Research Institute of Germans Trias i Pujol Foundation(IGTIP). Ctra. de Can Ruti /Camí de les escoles s/n, 08916, Badalona, Spain.

³ Center for Language and Speech Technologies and Applications (TALP), Technical University of Catalunya (UPC), Jordi Girona, 1-3, S112, Campus Nord, Barcelona, Spain.

⁴Escola Superior Politècnica Tecnocampus Mataró. Spain Phone Number: 34 93 169 65 01

Running head: Tuberculine test measured by Infrared Thermography

Word Count: 3046

Keywords: Tuberculine test, Infrared Thermography

29 **Corresponding author: Dr José Antonio Fiz**

30

31 **ABSTRACT**

32

33 Setting: The infection with *Mycobacterium tuberculosis* gives a delayed immune
34 response, measured by the tuberculine skin test. We present a new technique for
35 evaluation based on automatic detection and measurement of skin infrared emission.

36 Design: 21 subjects (57.0 ± 17.8 yr), (7/14, M/F) with suspected tuberculosis
37 contact were examined with an IR thermal camera, 48 hours after skin injection.

38 Results: In 15 subjects, IR analysis was positive for tuberculine test. Mean
39 temperature of injection area was higher, around 1 °C, for the positive group (36.0 ± 0.3
40 °C positive group; 35.2 ± 1.7 °C negative group, $p<0.001$, Non parametric U Mann-
41 Whitney Test).

42 Conclusion: IR may represent an improved estimation of tuberculosis infection,
43 given that it does not depend on reader variability and measures the increase of heat
44 irradiation produced by the allergic tuberculine response.

45

46

47

48

49

50

51

52

53

54

55

56

57

58

59

60

61

62

63

64

65

52 **INTRODUCTION**

53 According to the World Health Organization, two billion people are infected
54 with the tuberculosis (TB) bacilli¹. It is estimated that every year eight million new
55 cases appear. TB is a contagious disease not totally under control with great differences
56 between rich and poor countries². The diagnosis of TB is based on the interpretation of
57 a skin immunologic reaction. The infection with *Mycobacterium tuberculosis* gives a
58 delayed immune response, measured by the tuberculin skin test (TST)³. This consists of
59 the intradermal injection of tuberculin purified protein derivative (PPD) and
60 measurement of the resulting reaction. The induration size, measured in millimeters,
61 indicates if the test result is negative or positive. Palpation and pen methods have been
62 typically applied to measure the PPD reaction, but the measurement depends on the
63 subjective interpretation of the reaction area^{4,5}. New technologies are currently being
64 developed to improve the sensitivity and specificity of the TB diagnosis⁶.

65 In this study, we present a new technique for the evaluation of the tuberculine
66 reaction based on the automatic detection and measurement of infrared (IR) emission of
67 inflammatory effects produced by tuberculine immune response. IR thermal imaging is
68 a noninvasive technique for monitoring temperatures and is widely applied in
69 medicine^{7,8}. The IR radiation increases due to inflammatory processes, such as that in
70 the tuberculine reaction. An increased IR radiation is most likely caused by elevated
71 blood flow, metabolic activity, and inflammatory reactions⁹. Therefore IR thermal
72 imaging can be used to measure the rise in temperature due to an inflammatory process,
73 which causes the increase of the blood flow with vascular dilatation, blood proteins and
74 cellular extravasations¹⁰. PPD inflammatory response is characterized by edema,
75 leukocyte lymphocyte-mononuclear infiltration, and erythrocyte extravasation in the
76 dermis and epidermis¹¹. Our hypothesis in the present work was that intradermal

1
2
3
4
5
6
7
8
9
10
11
12
13
14
15
16
17
18
19
20
21
22
23
24
25
26
27
28
29
30
31
32
33
34
35
36
37
38
39
40
41
42
43
44
45
46
47
48
49
50
51
52
53
54
55
56
57
58
59
60
61
62
63
64
65

77 inflammatory PPD reaction produced an increase in the temperature of the injected area,
78 which could be measured by IR thermal imaging, and the features extracted from the
79 resulting IR images after applying digital image processing techniques, helped to
80 improve the reliability in the TB diagnosis.

81

1
2
3
4
5
6
7
8
9
10
11
12
13
14
15
16
17
18
19
20
21
22
23
24
25
26
27
28
29
30
31
32
33
34
35
36
37
38
39
40
41
42
43
44
45
46
47
48
49
50
51
52
53
54
55
56
57
58
59
60
61
62
63
64
65

82 MATERIAL AND METHODS

83 Ethics Statement

84 The study was conducted in the Respiratory Function Laboratory at HUGTIP,
85 from February- September 2014, and approved by the hospital's Human Research and
86 Ethics Committee. All participants came from pulmonology dept to discard tuberculosis
87 contact and gave written informed consent, following the World Medical Association's
88 Declaration of Helsinki on Ethical Principles for Medical Research Involving Human
89 Subjects.

90 Mantoux tuberculin skin test

91 The Mantoux tuberculin skin test (TST) was performed in all subjects by
92 intradermal injection of 0.1 ml of tuberculine purified protein derivative (PPD)
93 (Tuberculina PPD Evans 2 UT/0.1 ml, UCB Pharma S.A., Madrid, Spain) in the anterior
94 forearm. First, the reading of the Mantoux TST was manually performed 48 hours
95 following the skin injection³ by inspection, palpation, and measurement of the
96 induration. An induration size greater than 0.5 cm was considered to be a positive TST
97 result. A technician with more than 20 years experience in TST lecture has made all
98 TST test¹².

99 IR thermal imaging

100 The size of the induration was also measured by IR thermal imaging. Subjects
101 remained in the laboratory room for at least 15 minutes to achieve thermal equilibrium.
102 Temperature, humidity and air circulation were all controlled. Laboratory temperature
103 was maintained between 23 ± 1 °C, and humidity was around 50%. Subjects were
104 requested not to consume hot drinks or food for at least an hour before image session,
105 nor use any skin preparations such as creams or talcum powder. Emissivity of the skin

106 was assumed at a value of 0.98 ± 0.01 . There was no ceiling air filter. The lighting in
107 the laboratory was maintained at wavelengths longer than 1 micron.

108 The IR thermal images were obtained from the anterior surface of the forearm of
109 each subject, using a TiR32 Fluke Camera (2009 Fluke Corporation USA; 320x240
110 Focal plane array; 0.01 C° Noise Equivalent Temperature Difference; 8-14 μm spectral
111 range). The IR thermal camera was installed on a tripod with a fluke compact photo-
112 movie. The distance between the camera focus and the forearm was 40 cm. The forearm
113 was placed on a black foam cushion over a wooden table, with the anterior surface
114 facing the camera focus. To have a reference distance, we placed a 24 mm diameter
115 coin below the area to be measured. The detection of that reference object allowed us to
116 convert pixels to millimeters (Figure 1). The image acquisition and storage were made
117 with the SmartView® software. Each image was exported in JPG format. Moreover, the
118 temperature measurements were transferred to a text file.

119 **IR image processing**

120 The IR image processing was performed using Matlab 2014b and following the
121 scheme shown in Figure 2. Each text file containing the temperature data of an IR image
122 was imported in a 2D numerical array (*temp*). As IR images had different temperature
123 ranges, each *temp* array was scaled, as in (1), in order to have values between 0 and 1,
124 thus obtaining the gray scale image *temp_n* (Figure 3-a).

$$125 \quad temp_n = \frac{temp - T_{min}}{T_{max} - T_{min}} \quad (1)$$

126 T_{min} and T_{max} are the minimum and the maximum temperatures in *temp*
127 respectively. After obtaining the gray scale image *temp_n*, we detected the reference
128 object of known size that was present in the image in order to obtain the conversion

1
2
3
4
5
6
7
8
9
10
11
12
13
14
15
16
17
18
19
20
21
22
23
24
25
26
27
28
29
30
31
32
33
34
35
36
37
38
39
40
41
42
43
44
45
46
47
48
49
50
51
52
53
54
55
56
57
58
59
60
61
62
63
64
65

129 factor from pixels to millimeters. For that purpose, we first applied the Canny edge
130 detector to the normalized image *temp_n* (Figure 3-b). Then, since the reference object
131 was a circle, we used the circular Hough transform to detect its position and match its
132 edge (note that the Hough transform can be adapted to detect specific shapes in an
133 image)¹³. As the radius in millimeters of the reference object was known, we were able
134 to calculate the conversion factor to express measured lengths in millimeters (Figure 3-
135 c).

136 The temperature in the forearm area was much higher than the temperature
137 outside the forearm area (air). Therefore, the values of all pixels in the forearm area
138 were in the upper range of the scaled *temp_n* image. In order to clarify the differences
139 between the internal pixels of the forearm area, we applied an intensity transformation
140 to *temp_n*. All pixels below 0.5 were set at 0, whereas pixels in the range 0.5-1 were
141 expanded to the range 0-1, thus obtaining the *temp_e* image (Figure 3-d). The difference
142 between the PPD reaction area and the rest of the forearm was more noticeable in
143 *temp_e* than in *temp_n*.

144 The segmentation algorithm searched two different regions: region 1 (PPD
145 reaction area) and region 2 (erythema). A region growing method was used for the
146 image segmentation. Assuming that the PPD reaction area (region 1) was near the
147 image center, the first seed pixel was the pixel with the maximum temperature ($P_{T_{max}}$)
148 inside a centered rectangle area. A binarization was applied to the image *temp_e*. Pixels
149 of the surface of the forearm were retained (set at 1) and pixels outside the forearm (air)
150 were rejected (set at 0), thus obtaining the *temp_b* binary image (Figure 3-e). Then, a
151 5x5 cm square, which was centered at $P_{T_{max}}$, was selected as the analysis area mask.

152 Having found the first seed point and defined the analysis area, the region
 153 growing algorithm was applied to $temp_e$ by means of the following iterative procedure
 154 until convergence to a fixed point was reached. At each iteration, new sub-regions 1 and
 155 2 were grown from a new seed point, by adding in neighboring pixels according to each
 156 sub-region membership criterion. First, sub-region 1 was grown by adding in
 157 neighboring pixels that met the criterion in (2).

$$158 \quad -A * Th1 < \min S_1(i,j) < Th1 \rightarrow S_1(i,j) = reg_mean_1 - temp_e(i,j) \quad (2)$$

159 The parameter reg_mean_1 was the mean value of all pixels included in the whole
 160 region 1, $temp_e(i,j)$ was the intensity value of a neighboring pixel, $S_1(i,j)$ was the
 161 membership criterion of a neighboring pixel, $Th1$ was the threshold used to either
 162 include or not a neighboring pixel in sub-region 1, and A was the scale factor of $Th1$ to
 163 define the lower limit of $S_1(i,j)$. When there were not neighboring pixels meeting the
 164 criterion defined in (2), a new criterion, as defined in (3), was used to add in
 165 neighboring pixels to sub-region 2.

$$166 \quad \min(|S_2(i,j)|) < Th2 \rightarrow S_2(i,j) = reg_mean_2 - temp_e(i,j) \quad (3)$$

167 The parameter reg_mean_2 was the mean value of all pixels included in the whole
 168 region 2, $temp_e(i,j)$ was the intensity value of a neighboring pixel, $S_2(i,j)$ was the
 169 membership criterion of a neighboring pixel, and $Th2$ was the threshold used to either
 170 include or not a neighboring pixel in sub-region 2. When no neighboring pixels met the
 171 criterion defined in (3), a new seed point was selected and a new iteration started. Each
 172 new seed point had to meet the criterion defined in (2) and be at a maximum distance of
 173 15mm from the sub-region 1 obtained in the first iteration.

174 After the region growing process finished, when no new seed points existed,
 175 regions 1 and 2 were formed by a set of sub-regions 1 and 2, respectively (Figure 3-f).
 176 The maximum length of both region 1 and region 2 were calculated as the sum of the
 177 maximum length of their corresponding sub-regions (Figures 3-g and 3-h). The
 178 background area was calculated by removing the pixels belonging to either region 1 or
 179 region 2 from the analysis area mask. Then, the area (mm²), the minimum, the
 180 maximum, the mean, and the standard deviation temperatures (°C) were calculated
 181 either for region 1, region 2, and the background.

182 Finally, the region 2 was merged with the background if the following criterion
 183 was met:

$$t_{\text{mean}2} - t_{\text{std}2} - t_{\text{mean}3} - t_{\text{std}3} \leq 0.3 \quad (4)$$

185 where $t_{\text{mean}k}$ and $t_{\text{std}k}$ ($k = 2,3$) were the mean and standard deviation
 186 temperatures of region 2 and background, respectively. Furthermore, region 1 was
 187 merged with region 2 and the background if criterion defined in (4) and the following
 188 criteria were met:

$$t_{\text{mean}1} - t_{\text{std}1} - t_{\text{mean}23} - t_{\text{std}23} \leq 0.25 \quad (5)$$

$$t_{\text{mean}1} - t_{\text{std}1} - t_{\text{mean}2} - t_{\text{std}2} \leq 0.3 \text{ or } t_{\text{mean}2} - t_{\text{mean}3} \geq 0 \quad (6)$$

191 where $t_{\text{mean}k}$ and $t_{\text{std}k}$ ($k = 1, 23, 2, \text{ or } 3$) were the mean and standard deviation
 192 temperatures of region 1, region 2+background, region 2, and background, respectively.
 193 In those cases, only a background area was obtained as the final result of the image
 194 segmentation. Therefore, no reaction area was found and the test was negative. A
 195 negative/ positive segmentation indicated an IR negative/ positive result respectively.
 196 Also, for an expert in IR imaging that made all lectures of patient IR image, the non

197 existence of significant geometric IR color differences in the injection area was
198 classified as a negative result.

199 Statistics results were made by means of SPSS soft. Parametric and non
200 parametric tests were applied to observe the differences between groups. A Bland-
201 Altman plot and the Kappa Statistic were also applied to see the inter-observer variation.

202 **RESULTS**

203

204 Table 1 expresses the anthropometric characteristics of 21 subjects (7/14 M/F)
205 suspected of tuberculosis contact. Mean age was 57(17.9) years. Six had a positive PPD
206 lecture (more than 5 mm of papule). In 15 subjects IR analysis was positive for
207 tuberculine test.

208 Positive reaction of the IR visual examination was identified as one or more
209 central geometric images with circular, elliptic or with more irregular contours, easy to
210 differentiate from the rest of the IR surface (Figure 1). A higher temperature of this area
211 appeared with a more intense color respect to the neighboring (blue to red colour scale).
212 In subjects with a negative PPD test these characteristics were not evident in the IR
213 image. Only one subject with negative PPD reaction presented a IR positive
214 characteristic image.

215

216 Table 2 depicts IR parameters for the two groups of subjects: Group 1 with a
217 positive IR image (15 subjects) and Group 2 with negative IR reaction (6 subjects).
218 Mean, min, and maximum temperatures were higher for group 1 than group 2.
219 Differences for mean temperature were around 1 °C between both groups. These
220 parameters were higher in area 1 than area 2 for group 1 and there were not significant
221 differences from group 2. Differences for group 1 were around 0.5 °C between area 1
222 and area 2.

223 Regression coefficient between diameter of area 1 measured by exploration and
224 IR analysis was $R=0.8$, $R^2=0.64$, constant =6.13, coefficient beta=0.8, $p<0.001$. for all
225 subjects with a positive PPD (14). Mean difference of diameter measured by PPD
226 examination and IR analysis was around 1.4 mm (-12.6 to 5.5).

1
2
3
4
5
6
7
8
9
10
11
12
13
14
15
16
17
18
19
20
21
22
23
24
25
26
27
28
29
30
31
32
33
34
35
36
37
38
39
40
41
42
43
44
45
46
47
48
49
50
51
52
53
54
55
56
57
58
59
60
61
62
63
64
65

227 A Bland-Altman plot compares two assay methods. It plots the difference
228 between the two measurements on the Y axis, and the average of the two
229 measurements on the X axis (figure 4). Differences between diameter of induration
230 measured by exploration of PPD and IR image analysis of area 1 were into the 95%
231 limits of agreement (mean bias plus or minus 1.96 times its SD). The bias is computed
232 as the value determined by one method minus the value determined by the other
233 method. Bias was 1.4. and SD of Bias was 5.25. 95% limits of agreement were from -
234 8.9 to 11.7.

235 Inter-observer variation was measured by The Kappa Statistic, between
236 exploratory lecture of PPD and IR image analysis (Table 3). The agreement was 0.89
237 (almost perfect 0.81-0.99. Kappa Index).

238
239 **DISCUSSION**

240 The authors studied the skin tuberculine reaction in 21 tuberculosis contacts by
241 infrared emission image analysis and compared it with classical tuberculine examination.
242 Fourteen subjects with a tuberculin reaction size more than 5 mm had an IR positive
243 image reaction. Six subjects with negative tuberculin test had also a negative IR image.
244 One contact with a negative tuberculin test had a positive IR image. The diameter of
245 the IR reaction was higher than the diameter measured by skin examination.

246 Infrared imaging has been extensively applied in medicine since the 1960's.
247 Detection of peripheral vascular disorders and breast cancer are some
248 examples^{7,14,15,16,17}. In areas affected by a inflammation process characterized by
249 arteriolar capilar and venula dilatation with inflammatory infiltrate there is an increase
250 in an increasing of eat¹⁰. IR is able to detect skin temperature differences as low as 0.1

1
2
3
4
5
6
7
8
9
10
11
12
13
14
15
16
17
18
19
20
21
22
23
24
25
26
27
28
29
30
31
32
33
34
35
36
37
38
39
40
41
42
43
44
45
46
47
48
49
50
51
52
53
54
55
56
57
58
59
60
61
62
63
64
65

251 C°¹⁸. These properties had been applied in several medical cases as control of bar
252 infection¹⁹, replacement of total knee²⁰ and acne treatments^{21,22}.

253 The current measurement of tuberculine reaction is the subjective measure of
254 skin induration by tact. However, the reading of induration could be a potential error
255 source⁵. Margins of the induration are difficult to find independently of technique
256 (ballpoint-pen, palpation)⁴. On the other hand, it could be a subcutaneous inflammation
257 due to the tuberculine reaction but not evident by palpation as a false negative result or
258 doubtful lecture⁴. In this case, skin IR emission could be more sensible than a simple
259 examination. Histopathologic pattern of human intracutaneous tuberculine reaction was
260 described by Kuramoto²³ and more recently by Haholu¹¹. These reactions take place in
261 the epidermis and dermis. These cellular infiltrations with an extensive vascular
262 component (vasodilatation, edema exudation) are responsible for an increase in the heat
263 generation on the injection place that can be measured by IR camera¹⁰. Changes from
264 0.2 to 2 °C have been demonstrated in inflammatory dermatologic processes^{20,24,25}.

265 We observed a significant difference in the mean temperature between the
266 central segmented IR area and window hand area at around 1 C°. This temperature was
267 above that measured in healthy subjects⁸. In addition, the difference between the central
268 and surrounding area temperatures was significant, around 0.5 C°. A higher production
269 of heat indicates different inflammatory events in the same way that the small
270 indurations tact is different from the skin eritema area. Infection with M tuberculosis
271 causes a cell-mediated immune response leading to sensitized T lymphocyte²⁶.
272 Intradermal injection of PPD evokes a delayed hyper sensibility response mediated by
273 sensitized T cells that produces a skin induration²³. Erythema multiform and spongiotic
274 dermatitis are more related with PPD score based on the induration area. The most

1
2
3
4
5
6
7
8
9
10
11
12
13
14
15
16
17
18
19
20
21
22
23
24
25
26
27
28
29
30
31
32
33
34
35
36
37
38
39
40
41
42
43
44
45
46
47
48
49
50
51
52
53
54
55
56
57
58
59
60
61
62
63
64
65

275 frequent, basal spongiotic dermatitis, is characterized by edematous changes in the
276 epidermis and mononuclear exocytosis. In addition, the erythema multiform type has an
277 important component of edema with erythrocyte extravasations. In consequence we
278 believe that marked edema as a consequence of a prolonged vasodilatation with cellular
279 extravasations are responsible for increased temperature in the central area. This fact is
280 shown by an increase of irradiated heat as observed in other inflammatory diseases¹⁰.

281 One important finding of the current work was that one subject with a negative
282 PPD had a positive reaction to the IR analysis. The possibility that PPD shows false
283 negatives has been previously reported²⁷. An immune compromised state (HIV infection)
284 or immunologic-suppression and booster phenomenon may lead to false negative
285 results²⁷. Methodological technical causes such as sub-dermic, superficial injection with
286 an easy rupture of the vesicle, as well as a subjective interpretation caused by inter-
287 reader variability could constitute other causes of false negative results⁵. In fact, there is
288 a 10% rate of false negative PPD's in hospitalized patients, increasing to 50% in cases
289 of disseminate tuberculosis²⁶. In consequence, IR could substantially improve the
290 sensibility in these cases. We are not able to add any new data regarding false positive
291 cases, which is an intrinsic problem of the tuberculine reaction. IR only provides
292 information about local skin inflammatory reactions regardless of the kind of
293 inflammation or germ-causing disease. New immune based tests such as interferon- γ
294 release assay or POC technologies could increase the sensibility and specificity of
295 tuberculosis diagnostic⁶.

296 Several issues related to methodology of the present paper must be addressed.
297 First, the reduced group of patients has not permitted us to draw general conclusions,
298 but in the present work a positive IR reaction was observed in all TST manual lecture

1
2
3
4
5
6
7
8
9
10
11
12
13
14
15
16
17
18
19
20
21
22
23
24
25
26
27
28
29
30
31
32
33
34
35
36
37
38
39
40
41
42
43
44
45
46
47
48
49
50
51
52
53
54
55
56
57
58
59
60
61
62
63
64
65

299 except in one and also negative IR reaction was observed in all negative TST test. In
300 conclusion, although it needs a larger sample to extract definitive conclusion, we think
301 that these results induce to perform a multicentre study that will permit the definitive
302 generalization of present procedure. On the other hand, infrared reading was made
303 following the guidelines for standardization in Medical Thermography¹⁷. We think that
304 this procedure could be applied with no restrictive conditions that will permit to use more
305 simple elements as an IR mobile-camera in different spaces for its general use.

306 Worth to mention that our previous work²⁸ revealed that thermal imaging
307 provides complementary information to visual imaging, from an information theory
308 point of view.

310 **Conclusion**

311 IR may represent an improved estimation of tuberculosis infection, given that,
312 IR reading does not depend on reader variability and only measures the increase of heat
313 irradiation produced by the allergic tuberculin response, which is the IR physical
314 principle that could be objectively measured.

315 **REFERENCES**

- 316 1. WHO. Report 2004. Global tuberculosis control. Surveillance. Planning.
317 Financing. WHO edit. Ginebra 2004.
- 318 2. Gallardo J, Ramos A, Jara B, Ancochea J. Tuberculosis. In Manual de
319 Neumología Clínica (2º edition). Diez JM, Alvarez-Sala R editors (ERGON).
320 2009 193:213

- 1
2
3
4
5
6
7
8
9
10
11
12
13
14
15
16
17
18
19
20
21
22
23
24
25
26
27
28
29
30
31
32
33
34
35
36
37
38
39
40
41
42
43
44
45
46
47
48
49
50
51
52
53
54
55
56
57
58
59
60
61
62
63
64
65
3. American Thoracic Society and Centers for Disease Control And Prevention:
Diagnostic standars and classification of tuberculosis in adults and children.
Am J Respir Crit Care Med 2000 161:1376.
 4. Bouros D, Zeros G, Panaretos C, Vassilatos C, Siafakas N. Palpation vs pen
method for the measurement of skin tuberculin reaction (Mantoux test). Chest,
1991 99:416-9.
 5. Pouchot J, Grosland A, Collet C. Coste J, Esdaile JM, Vinceneux P. Reliability of
tuberculin skin test measurement. Ann Intern Med 1997 126:210-4.
 6. Pai M, Minion J, Sohn H, Zwerling A, Perkins M.D. New technologies for
tuberculosis diagnosis. Clin Chest Med 2009 30:701-716.
 7. Bagavathiappan S, Sarananan T, Philip J, Jayakumar T Ph J, Baldev R,
Karunanithi R, Panicker T.M.R, Korath M.P, Jagadeesan K. Infrared thermal
imaging for detection of peripheral vascular disorders. J Med Phys 2009 34:43-
47.
 8. Ring EFJ, Ammer K. The technique of infrared imaging in medicine.
Thermology International 2000 1:7-14.
 9. Schaefer A.L, Cool N, Tessaro S.V, Deregt D, Desroches G, Dubeski P.L,
Tong A.K.W, Godson D.L. Early detection and prediction of infection using
infrared thermography. Can J Anim Sci 2004 84:73-80.
 10. Ring F.E, Ammer K, Thermal imaging in diseases of the skeletal and
neuromuscular systems. In Medical infrared imaging. Edited by N.A. Dinkides,
J.D. Bronzino CRC, US. 2008:17-1.
 11. Haholu A, Ciftci F, Karabudak O, Kutlu A, Bozkurt B, Baloglu H. The
significance of histopathologic patterns in positive tuberculin skin test. Journal
of Cutaneous Pathology. 2008 35:462-465.
 12. De Souza-Galvao M.L, Latorre I, Altet-Gómez N, Jiménez_Fuentes, Milà C,
Solsona J, Seminario M.A, Cantos A, Ruiz-Manzano J, Dominguez J.

1
2
3
4
5
6
7
8
9
10
11
12
13
14
15
16
17
18
19
20
21
22
23
24
25
26
27
28
29
30
31
32
33
34
35
36
37
38
39
40
41
42
43
44
45
46
47
48
49
50
51
52
53
54
55
56
57
58
59
60
61
62
63
64
65

348 Correlation between tuberculin skin test and IGRAs with risk factors for the
349 spread of infection in close contacts with sputum smear positive in pulmonary
350 tuberculosis. *BMC. Infectious Diseases* 2014 14:258.

351 13. Gonzales R. C., Woods R. E. *Digital Image Processing*. New Jersey: Prentice
352 Hall; 2002.

353 14. Wang J, Chang KJ, Chen CY, Chien KL, Tsai YS, Wu YM, Teng YC, Shiht T.
354 Evaluation of the diagnostic performance of infrared imaging of the breast: a
355 preliminary study. *BioMedical Engineering Online* 2010 9:3.

356 15. Ring EFJ. Standardization of Thermal Imaging in Medicine: Physical and
357 Environmental factors in Thermal Assessment of Breast Health. Ed Gautherie
358 M, Albert E, Keith L, 29-36. MTP Press Ltd. Lancaster/Boston/The Hague.
359 1983.

360 16. Engel JM, Cosh JA, Ring EFJ, Page DP, Van Waes P, Shoenfeld D.
361 Thermography in Locomotor Diseases- Recommended Procedure. *Eur J*
362 *Rheum Inflamm* 1979 2:299-306.

363 17. Clark RP, de Calcina-Goff M. Guidelines for Standardization in Medical
364 Thermography Draft International Standard Proposals. *Thermologie Österreich*
365 1997 7:47-58.

366 18. Cetingül M, Herman C. Identification of subsurface structures from the transient
367 thermal response and surface temperature measurements, in: Proceedings of
368 the 5th European Thermal-Sciences Conference 18-22 May, Eindhoven 2008:
369 1219-1222.

370 19. Fujita K, Noguchi M, Yuzurika Sh, Yanagisama D, Matsuo K. Usefulness of
371 infrared thermal imaging camera for screening of postoperative surgical site
372 infection after the nose procedure. *Case Rep Surg* 2013:946156.

1
2
3
4
5
6
7
8
9
10
11
12
13
14
15
16
17
18
19
20
21
22
23
24
25
26
27
28
29
30
31
32
33
34
35
36
37
38
39
40
41
42
43
44
45
46
47
48
49
50
51
52
53
54
55
56
57
58
59
60
61
62
63
64
65

373 20. Romariò CL, Logoluso N, Dell’Oro F, Elia A, Drago L. Telethermographic
374 findings after uncomplicated and septic total knee replacement. *Knee* 2012
375 19:193-7.
376 21. Padilla-Medina JA, León-Ordoñez F, Prado-Olivarez J, Vela-Aguirre N,
377 Ramirez-Agundis A, Diaz-Carmona J. Assessment technique for acne
378 treatments based on statistical parameters of skin thermal images. *Comput Biol*
379 *Med* 2004 47:36-43.
380 22. Herman C. The role of dynamic infrared imaging in melanoma diagnosis.
381 *Expert Rev Dermatol* 2013 8:177-184.
382 23. Kuramoto Y, Tagani H. Histopathologic pattern analysis of human
383 intracutaneous tuberculin reaction. *The American Journal of*
384 *Dermatopathology* 1989 11:329-337.
385 24. Van Netten JJ, Van Baal JG, Liu C, Cn der Jeijden F, Bus SA. INfrared
386 thermal imaging for automated detection of diabetic foot complications. *J*
387 *Diabetes Sci Technol* 2013 1:1122-9.
388 25. Han SS, Jung CH, Lee SC, Jung HJ, Kim YH. Does skin temperature
389 difference as measured by infrared thermography within 6 months of acute
390 herpes zoster infection correlate with pain level?.
391 26. Brodie D, Schluger N.W. The diagnosis of tuberculosis. *Clinics in chest*
392 *medicine* 2005 26:247-271.
393 27. Huebner RE, Schein MF, Bass Jr JB. The tuberculin skin test. *Clin Infect Dis*
394 1993 17:968-75.
395 28. Virginia Espinosa-Duró, Marcos Faundez-Zanuy, Jiri Mekyska, Enric Monte-
396 Moreno. A Criterion for Analysis of Different Sensor Combinations with an
397 Application to Face Biometrics. *Cogn Comput* (2010) 2:135–141
398

399
400
401
402
403

TABLE 1 ANTROPHOMETRIC CHARACTERISTICS OF SUBJECTS WITH SUSPECTED TBC

	Male			Female			
(M/F)	Age(ys)	Height(cm)	Weight(Kg)	Age(ys)	Height(cm)	Weight(Kg)	Total
All	57.0(17.8)	156.0(17.4)	70.0(20.1)	51.4(15.9)	155.8(8.1)	52(11.6)	21
Positive (6/9)	48.3(18.7)	172.5(5.9)	73.1(10.0)	45.2(13.8)	159.3(6.4)	64.9(8.7)	15
Negative (1/5)	32	189	97	62.4(14.3)	149.4(7.3)	64.7(16.9)	6

404
405
406
407
408

Table 1. Anthropometric values of 21 subjects with tuberculosis contact suspected . Positive and negative test responses were measured by infrared analysis (IR) with a term graphic IR camera. All a values are in mean(sd).

1
2
3
4
5
6
7
8
9
10
11
12
13
14
15
16
17
18
19
20
21
22
23
24
25
26
27
28
29
30
31
32
33
34
35
36
37
38
39
40
41
42
43
44
45
46
47
48
49
50
51
52
53
54
55
56
57
58
59
60
61
62
63
64
65

409

410 **TABLE 2. INFRARED LECTURE OF SUBCUTANEAU TUBERCULINE TEST IN**
411 **PATIENTS WITH SUSPECTED OF TUBERCULOSIS**

412

Group 1 (+) (15)	Area 1	Area 2	Area 3
Area mm²	0.96 (0.75)*+	6.71 (7.88)	17.17(7.76)
T min °C	35.93(0.85)*+	35.33(1.06)	33.52(1.11)
T max °C	36.34(0.78)*+	36.02(0.83)	35,82(1.08)
T mean °C	36.04(0.33)*+	35.57(0.96)	34,71(0.93)
Diameter mm	15.45(7.24) +	37.45(20.53)	
Group 2 (-) (6)	Area 1	Area 2	Area 3
Area mm²	7.54 (5.31)	5.71 (2.91)	6.27 (3.59)
T min °C	34.27(3.45)	34.17(1.77)	32.78(2.00)
T max °C	35.15(1.51)	35.07(1.61)	35.73(1.46)
T mean °C	35.18(1.68)	34.51(1.67)	34.58(1.48)

413

414

- * Signification level p<0.05. Non parametric U Mann-Whitney Test between Groups

415

416

- + Signification level p<0.05. Difference between area 1 and 2. Non parametric Wilcoxon Rang-sig test for the same group.

417

418

Group 1: Tuberculine lecture IR positive ; Group 2: Tuberculine lecture IR negative.

419

420

All values are in mean(sd)

421

422

423

424

425

426

TABLE 3. INTEROBSERVER AGREEMENT. TheKappa Statistic

		Exploratory lecture of PPD		
		Positive	Negative	Totals
IR image	Positive	14	1	15
	Negative	0	6	16
	Totals	14	7	21

427

428 **Kappa Statistic agreement between observed PPD exploration and IR image**
 429 **analysis in 21 subjects with TBC contact suspect.**

430 Absolute agreement= 0.95. Hope agreement= 0.57.

431 Kappa Index: 0.89. Standar error I.C 95% (0.67-1.1).

432

1
2
3
4
5
6
7
8
9
10
11
12
13
14
15
16
17
18
19
20
21
22
23
24
25
26
27
28
29
30
31
32
33
34
35
36
37
38
39
40
41
42
43
44
45
46
47
48
49
50
51
52
53
54
55
56
57
58
59
60
61
62
63
64
65

433 **FIGURE 1-IR images in a positive PPD test.**

434 Figure 1-1 is the photograph of the injection tuberculine area. We can observe a
435 higher IR intensity in the area of tuberculine injection (Figures 1-1, 1-3). Figure 1-2 is
436 a superposition of IR and colour photographic image. To have a reference distance, we
437 placed a 24 mm diameter coin below the area to be measured

438

439 **FIGURE 2 – Flowchart of the IR image processing algorithm.**

440 First, image *temp* was scaled, thus obtaining image *temp_n*. Then, the reference
441 object was detected (center and radius), which allowed us to calculate the conversion
442 factor from pixels to millimeters. Next, an intensity transformation was applied to
443 *temp_n*, thus obtaining image *temp_e*. A region growing segmentation algorithm was
444 applied to *temp_e* in order to obtain region 1, region 2, and the background. Finally,
445 some parameters are calculated for each region and these parameters were used to
446 decide if some region were merged or not.

447

448 **FIGURE 3-Different aspects of the image processing algorithm**

449 (a) *temp_n* image; (b) Edges detection by Canny's method; (c) *temp_n* image after
450 rejecting the internal pixels of the reference object; (d) *temp_e* image (white expansion)
451 and the analysis area (red square); (e) Analysis area mask; (f) PPD reaction area (white),
452 erythema (light gray), and background (dark gray); (g) PPD reaction area and its
453 maximum distance; (h) Erythema and its maximum distance; (i) Edges of the PPD
454 reaction area and the erythema.

455

1
2
3
4
5
6
7
8
9
10
11
12
13
14
15
16
17
18
19
20
21
22
23
24
25
26
27
28
29
30
31
32
33
34
35
36
37
38
39
40
41
42
43
44
45
46
47
48
49
50
51
52
53
54
55
56
57
58
59
60
61
62
63
64
65

456 **FIGURE 4. Bland-Altman plot**
457

458 A Bland-Altman plot compares two assay methods. It plots the difference
459 between the two measurements on the Y axis, and the average of the two measurements
460 on the X axis. In this case the two measures are: the diameter measured by manual
461 exploration of the PPD papula and the diameter of area 1 measured by IR image
462 analysis. The 95% limits of agreement are shown as two dotted lines.

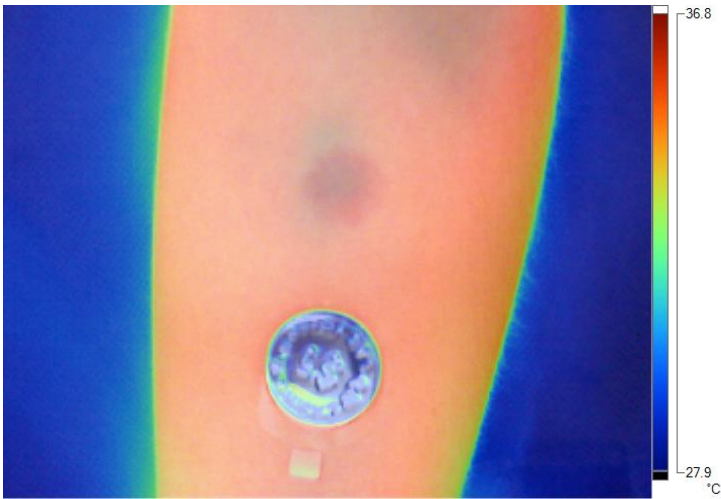
463

464

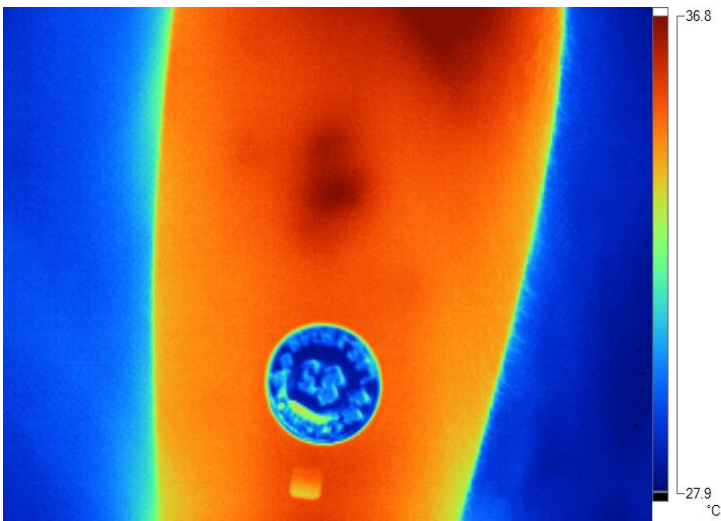
1
2
3
4
5
6
7
8
9
10
11
12
13
14
15
16
17
18
19
20
21
22
23
24
25
26
27
28
29
30
31
32
33
34
35
36
37
38
39
40
41
42
43
44
45
46
47
48
49
50
51
52
53
54
55
56
57
58
59
60
61
62
63
64
65



465



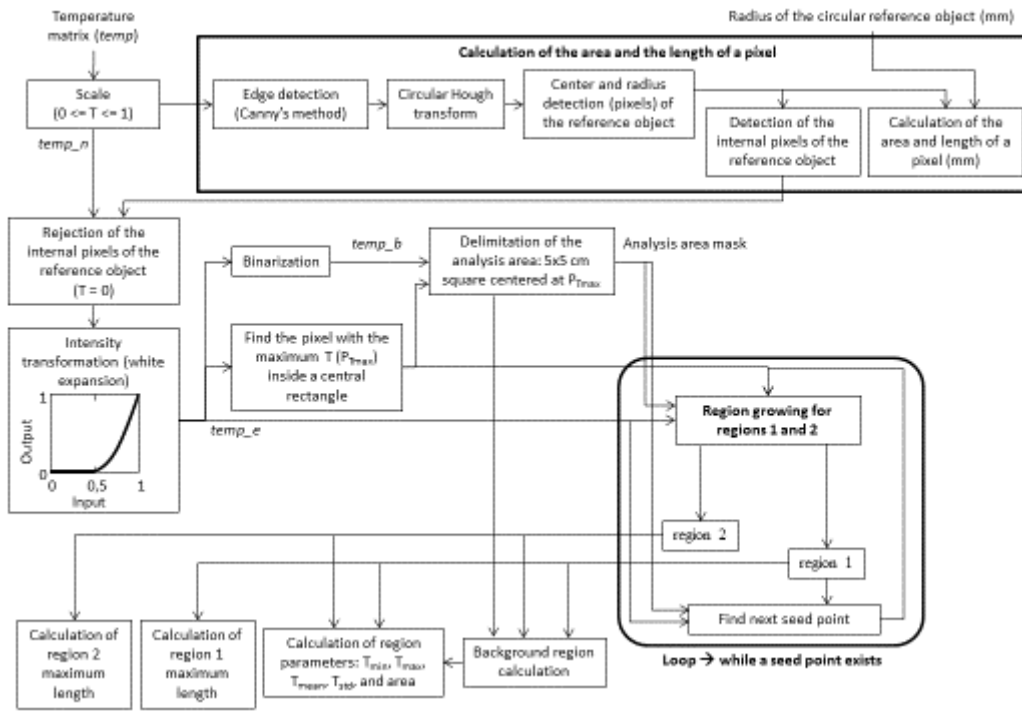
466



467

468 **FIGURE 1.**IR images in a subject with a positive PPD test

469



470
471
472 **FIGURE 2 . Flowchart of the IR image processing algorithm**

1
2
3
4
5
6
7
8
9
10
11
12
13
14
15
16
17
18
19
20
21
22
23
24
25
26
27
28
29
30
31
32
33
34
35
36
37
38
39
40
41
42
43
44
45
46
47
48
49
50
51
52
53
54
55
56
57
58
59
60
61
62
63
64
65

491
492
493
494
495
496
497
498
499
500
501
502

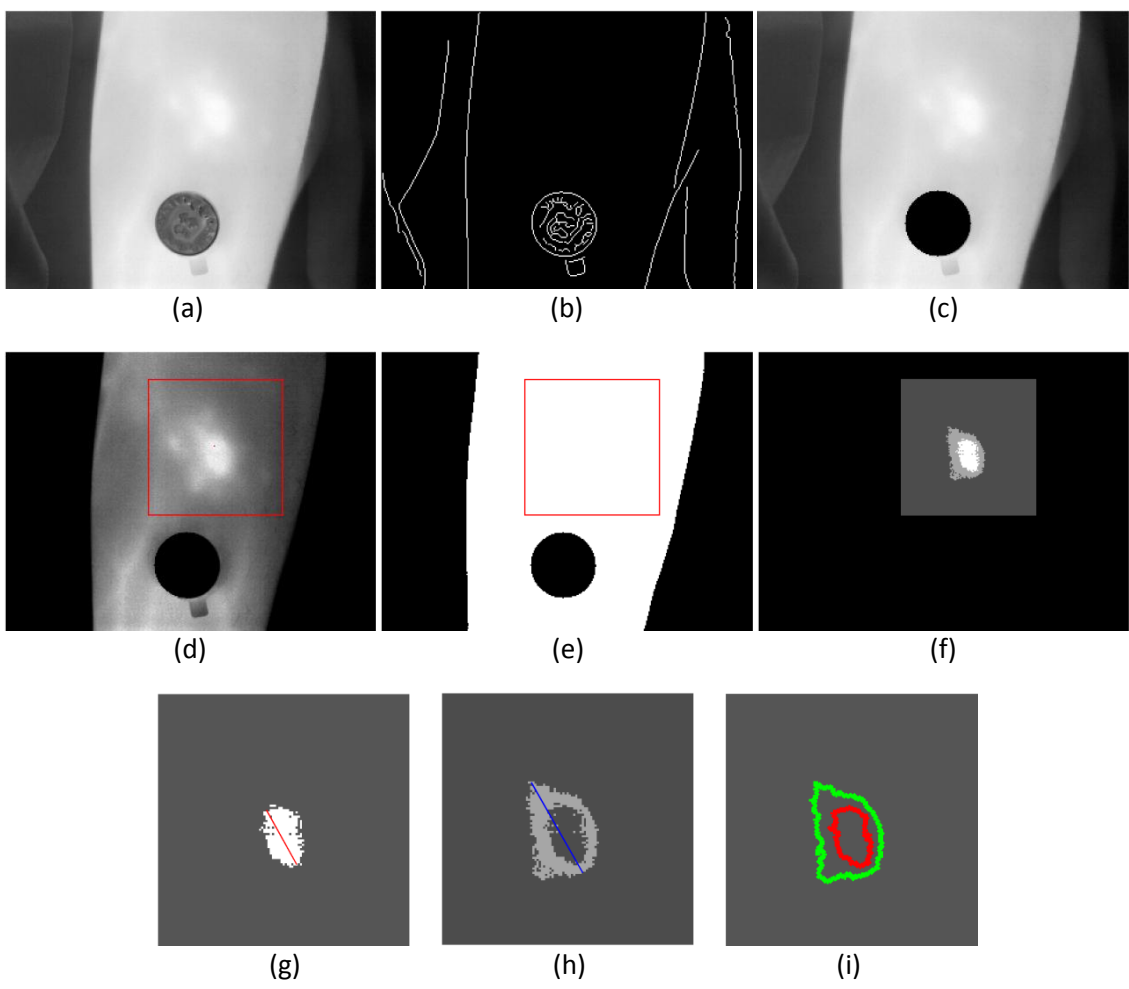
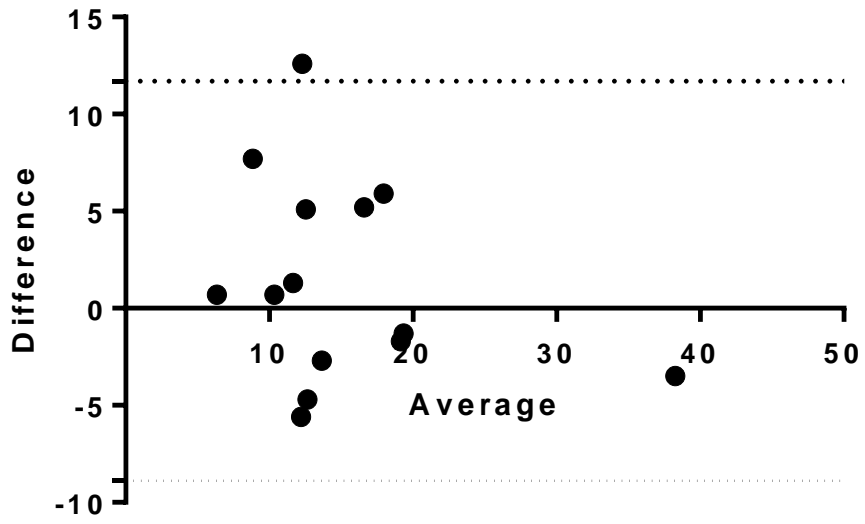


FIGURE 3. Different aspects of the image processing

algorithm

503

504



505

506

507

FIGURE 4. Bland-Altman plot

508
1 509
2 510
3 511
4 512
5 513
6 513
7 514
8 515
9 516
10 517
11 518
12 519
13 520
14 521
15 522
16 523
17 524
18 525
19 526
20 527
21 528
22 529
23 530
24 531
25 532
26 533
27 534
28 535
29 536
30 537
31 538
32 539
33 540
34 541
35 542
36 543
37 544
38 545
39 546
40
41
42
43
44
45
46
47
48
49
50
51
52
53
54
55
56
57
58
59
60
61
62
63
64
65

Declaration of conflict of interest

The authors state that they have no conflict of interest in the elaboration of this paper.

Acknowledgements

The authors wish to thank the nurses Rosa Gomez and Aurora Torrents for their special assistance.

AUTHOR’S CONTRIBUTIONS:

- José Antonio Fiz Fernández: inventor of procedure, design of the work; processed and automation of image analysis; analysis and interpretation of the data for the work; writing the article; guarantor of the paper.
- Manuel Lozano :Processed and automation of image analysis; analysis and interpretation of the data for the work; writing the article
- Enrique Monte Moreno: Analysis and interpretation of the data; writing the article; revision of the word.
- Marcos Faundez: IR support and revision of the word.
- Laura Rodriguez Pons: Clinical study of patient Inclusion
- Caroline Becker: Clinical study of patient Inclusion.
- Adela Gonzalez_Martinez: PPD test realization.
- Juan Ruiz Manzano. :Clinical study of patient Inclusion.